Lasso-grafting of macrocyclic peptide pharmacophores yields multi-functional proteins

Emiko Mihara
Osaka University
Satoshi Watanabe
Osaka University
Nasir Bashiruddin
University of Tokyo
Nozomi Nakamura
Osaka University
Kyoko Matoba
Osaka University
Rumit Maini
Arizona State University The Biodesign Institute
Yizhen Yin
University of Tokyo
Katsuya Sakai
Kanazawa University https://orcid.org/0000-0002-0443-1786
Takao Arimori
Osaka Univ https://orcid.org/0000-0002-6063-5572
Kunio Matsumoto
Kanazawa University https://orcid.org/0000-0002-6532-4482
Hiroaki Suga
University of Tokyo https://orcid.org/0000-0002-5298-9186
Junichi Takagi (takagi@protein.osaka-u.ac.jp)
Osaka University https://orcid.org/0000-0002-1219-475X

Article

Keywords: Lasso-grafting, multifunctional recombinant proteins, Random non-standard Peptides Integrated Discovery system(RaPID)

Posted Date: October 7th, 2020

DOI: https://doi.org/10.21203/rs.3.rs-85705/v1

Version of Record: A version of this preprint was published at Nature Communications on March 9th, 2021. See the published version at https://doi.org/10.1038/s41467-021-21875-0.

Abstract

Engineering of multifunctional recombinant proteins are a promising approach for devising next-generation proteinous drugs that engage specific receptors on cell(s), but it often requires drastic modifications of the parental protein scaffolds, e.g., additional domains at the N/C-terminus (or termini) or replacement of a domain to another. A discovery platform system, called RaPID (Random non-standard Peptides Integrated Discovery) system, has enabled for a rapid discovery of small de novo macrocyclic peptides that bind a target protein with high binding specificity and affinity. Taking the advantage of such exquisite properties of the RaPID-derived peptides, here we show that their pharmacophore sequences can be implanted to a surface-exposed loop or loops of recombinant proteins and maintain not only the parental peptide binding function(s) but also the host protein function. By applying this method, referred to as lasso-grafting, many different proteins including IgG and serum albumin could be endowed with binding capability toward various receptors, allowing us to quickly formulate bi-, tri-, and even tetra-specific binder molecules. Moreover, lasso-grafting of a receptor-targeting peptide to capsid proteins of adeno-associated virus (AAV) has generated engineered AAV vectors that can infect cells solely dependent on the targeted receptor.

Background

Macrocyclic peptides represent a class of synthetic compounds that is rapidly gaining attention as a new drug modality, particularly in the therapeutic intervention of protein-protein interfaces (PPIs)[1,2]. Compared to the traditional small molecule drugs, they generally have large binding footprints on the surface of a target protein comparable to that of typical antibody, leading to the high specificity and affinity despite their small to medium size (MW in the range of 1,000 - 3,000 Da). By using the mRNA-display in combination with genetic code reprogramming, referred to as the RaPID (Random non-standard Peptides Integrated Discovery) system, we have isolated and reported many *de novo* macrocyclic peptide binders against various proteins from a pool of random sequences consisting of more than 10^{12} members (Figure 1a)[3,4]. Such peptides generally exhibit exquisite binding specificity and high affinity toward the target, and have proven to be highly useful in applications such as receptor antagonist or agonist, crystallization chaperone, and imaging/detection tool [5-9]. Despite the fact that the method offers an extraordinary speed to identify potent species, the macrocyclic peptides are not necessarily ready for drug use because they often suffer from unpredictable pharmacokinetics and bioavailability [10]. If one can copy a rapidly identified “pharmacophore(s)” on macrocyclic peptides and make it (or them) an integral part of a natural human protein, that would make a more reliable drug format bearing the merit of both macrocycles and proteins.

In this study, we show that the binding ability of the RaPID-derived macrocyclic peptides can be maintained when the thioether ring-closure moiety is replaced by a self-folding protein domain. Unexpectedly, this does not demand any special protein engineering efforts and can be achieved by simply taking the internal sequence of a RaPID peptide and simply inserting it into a surface-exposed

loops of a wide range of proteins. By applying this technology, many different proteins including IgG and serum albumin could be endowed with binding capability toward various receptors, allowing us to quickly formulate bi-, tri-, and even tetra-specific binder molecules. Moreover, this extraordinarily facile method has enabled us to generate a target-specific AAV vector that can infect cells solely via the lasso-peptide–receptor interaction.

Results

The RaPID selection methodology is a powerful platform that can derive target-specific high-affinity macrocyclic peptides from a pool of vast number of candidate peptides. Although the library design obligates that all peptides are cyclized by a thioether bond [11], this ring-closure may be replaced by other types of chemical structure, because the target-binding is generally mediated by a set of correctly positioned amino acid residues from the internal sequence (Figure 1a, left). Most importantly, our available X-ray structures of co-crystals of peptide-protein have indicated that the peptides are self-folded albeit a wide range of tertiary structures appeared to be available [12]. We hypothesized that this "pharmacophore" structure can be maintained if a close apposition of the N- and C-termini of the peptide is reinforced by fusing a protein domain (Figure 1a, right (i)). We first searched for a dimeric protein suitable for this fusion topology and found uteroglobin (UG). UG is a small secreted homodimeric protein comprising two ~70 residue chains, which exchange their N- and C-termini in a juxtaposed fashion with a stabilizing disulfide-bridge (Fig. 1b) [13]. To test the hypothesis if the core sequence of a RaPID peptide displayed on a protein of choice could retain its binding function, we constructed an expression plasmid containing two UG monomers at both ends of linearized PB1m6 peptide (simply called m6 hereafter), a 17-residue macrocyclic peptide known to bind with human Plexin B1 (PlxnB1) at high affinity (Figure S1a)[6]. This "single-chain" version of UG homodimer connected by m6 (UG_2-m6) was expressed well in mammalian cells and purified from the culture supernatant by using the $(His)_6$ tag appended at the C-terminus (Figure S1b). A surface plasmon resonance (SPR) experiment showed that this UG_2-m6 retained the binding activity of parental m6 peptide toward PlxnB1 (Fig. 1c, Fig.S1c). Although the binding affinity of the UG_2-m6 was approximately 13-fold lower than that of the original cyclic peptide (Fig. 1c), this was mainly due to the slower on rate (k_{on}), which was naturally expected considering the reduction of the diffusion rate caused by the increase in the molecular size (2,031 Da for free peptide vs 18,506 Da for UG_2-fusion protein). As the k_{off} value remained unchanged (in fact, the grafted version showed 3-fold slower rate), intrinsic binding ability was virtually the same between UG_2-cyclized m6 and thioether-cyclized m6. We also tested that an affinity-matured variant of m6, m6A9, isolated recently by partially randomizing the internal sequence of m6 [Bashiruddin, submitted] exhibits the same property. When m6A9 was formulated in the same manner, UG_2-m6A9 also showed specific binding toward PlxnB1 with the k_{off} value similar to that of free peptide (Fig. 1c, Fig. S1d). We next applied the same UG_2-fusion strategy to different RaPID-derived peptides including another PlxnB1-binding peptide PB1m7 [6] and two MET-binding peptides aMD4 and aMD5 [5] (Table S1). All these UG_2-peptide fusions exhibited specific binding toward the respective targets with k_{off} values comparable to those of free peptides (Fig.1c and

Fig.S1f-h), confirming that the grafting compatibility is not a special property of PB1m6/m6A9 but is shared among distinctive RaPID-derived cyclic peptides with completely different sequences and target-dependencies. Interestingly, an UG_2-m6 mutant, where the ring-closing disulfide-Cys residues were mutated to Ser residues, showed binding kinetics very similar to that of the parental fusion (Fig. S1d and e), suggesting that the disulfide knot connecting the bottom of the loop may not be essential for the binding function.

The above observations motivated us to build another hypothesis. As the inserted peptide portion displayed on UG_2 (Fig. 1b, dotted line) is topologically equivalent to a loop protruding from a globular protein, the ring-closure could be achieved by simply inserting the peptide core motif into an open-cut point in the middle of a loop in arbitrary proteins, in a method referred to as lasso-grafting hereafter (Fig. 1a, right (ii)). In order to test this hypothesis, we chose 4 b-sandwich fold domains (10th FN-III module of human fibronectin, the first IgV domain of human carcinoembryonic antigen (CEA), the first IgV domain of signal regulatory protein alpha (SIRPa), and anti-GFP single domain antibody (VHH)) as the insertion scaffold. The internal peptide sequence of m6A9 or aMD4 were inserted into 2 sites (s1 or s2) both located at the tip of b-hairpin loops (Fig. 2a-d and Table S2), based on the assumption that such a topology would be ideal to maintain functional conformation of the parental macrocyclic peptides. When expressed as C-terminally Fc-tagged proteins, these peptide-inserted b-sandwich domains were not only secreted well, but also showed specific binding to the respective targets, PlxnB1 (for m6A9) and MET (for aMD4), in an immunoprecipitation-like pull-down assay (Fig. 3a–d), confirming that the lasso-grafting is compatible with various b-sandwich domains. We also found that the b-hairpin-rich Fc domain itself can accommodate peptide lasso-grafting at as many as 8 locations (Fig. 2e), all of which acquiring target binding ability of the parent RaPID peptide (Fig. 3e). Furthermore, the Fc-peptide fusions were able to bind to their target receptors expressed on cell surface (Fig. 4a and b). We next explored if protein domains other than the b-sandwich fold could be compatible with this strategy. We chose three types of globular proteins, all-a (human serum albumin, HSA, and human growth hormone, hGH), b-barrel (retinol binding protein, RBP), and a/b (alkaline phosphatase, ALP) fold topologies and constructed the respective fusions with the m6A9 and aMD4 peptides (a total of 18 constructs, Fig. 2f–i). Near-stoichiometric target binding ability was granted to 16 out of the 18 constructs (Fig. 3f–i). We conclude that the core motif of the high-affinity RaPID peptides, which are optimized functionally and conformationally when cyclized appropriately by juxtaposed N- and C-termini, can be grafted to a stably folded protein domain with a remarkably high success rate. To further evaluate the robustness of this method for the applicability to other peptide-target pairs, we lasso-grafted three distinctive thioether-macrocyclic peptide motifs against EGFR (A6-2f), TrkB (tkD5), and a6b1 integrin (IB8), isolated in our laboratory (Table S1), to the s8 site of the Fc protein. The FACS analysis of the peptide-Fc fusions revealed their specific binding ability to cells expressing the respective target receptor proteins (Fig. 4c-e). This strongly suggests that the RaPID-selected macrocyclic peptides can be rapidly formulated into various protein formats of choice.

The above proof-of-concept studies using the Fc domain stimulated us to apply the method of lasso-graft for more medically attractive protein scaffolds. We first applied it for generating multi-specific

antibodies, one of the emerging biological drug modalities. Since any IgG scaffold consists of a Fc region as a common structural domain and two Fab regions with highly variable antigen-binding sites, we envisioned that lasso-graft of the RaPID peptides to the Fc region of an IgG can readily add another binding property without disturbing the bivalent property of the Fab's antigen binding site. To test this idea, we chose three medically relevant antibodies, anti-neuropilin-1(Nrp1) YW64.3 [14], anti-PD-L1 avelumab [15], and anti-CD3 OKT3 [16], and lasso-grafted three representative RaPID peptides (m6A9, aMD4, and A6-2f) to their Fc region. FACS analysis revealed that each antibody retained the parental binding capacity toward the original antigen receptors expressed on cells (Fig. 5a-c, top-row panels), indicating that the lasso-grafted Fc-fusion did not disturb the Fab's function. Furthermore, these antibodies gained additional binding ability toward the second antigen, precisely emulating the binding specificity of the inserted peptide (Fig. 5a-c). In addition, lasso-grafting of multiple peptides onto anti-Nrp1 antibody using different Fc sites resulted in an incremental gain of binding specificity, ultimately enabling creation of an antibody with 1+3 binding specificities (Fig. 5a, the far-right panels labeled "triple"). It is extraordinary that one can formulate a quadruple binder antibody by simply "pasting" three peptide grafts onto an existing antibody, thanking to the presence of up to 8 grafting-compatible sites on the Fc portion (Fig. 2e). In this multi-specific antibody format, referred to as addbody hereafter, the bivalency of the binding functionality in Fc and that of the original antigen-binding site in two Fab regions are located on the opposite ends of the whole IgG molecule, suggesting its ability to simultaneously engage two antigens on opposing cell surfaces. In order to test the utility of our addbody format in such applications, the OKT3-based addbody grafted with MET-binding aMD4 peptide was incubated with MET-expressing CHO cells together with CD3-expressing Jurkat cells. The aMD4-bearing OKT3, but not the parent OKT3, clearly induced heterotypic cell-cell attachment (Fig. 5d), indicating that the addbody can efficiently bridge two specific cells in a manner similar to the bispecific antibodies used in the therapies for redirecting immune effector cells to tumor cells [17].

We next took advantage of the modularity of the lasso-graft method in changing the cellular tropism of adeno-associated virus (AAV), one of the most well-studied and promising gene-delivery vehicles. AAV is a small, naked icosahedral virus with 60-subunit capsid composed solely of a product of *Cap* gene [18], which harbors binding sites toward various cellular receptors, such as proteoglycans and AAVR [19]. Because these receptors are expressed on wide range of cells, AAV has intrinsic property of broad tropism, generally facing difficulties in delivering genes to a particular tissue(s) or organ(s). To solve this limitation, capsid engineering involving mutagenesis-based random screening and/or insertion of non-viral protein moieties into the capsid has been attempted yielding some successes [20-22], but problematically it is labor-demanding if one wishes to implant new specificity on AAV. On the other hand, the modularity of the lasso-grafting method would enable us to readily alter the specificity of AAV. We thus chose Cap loops for lasso-grafting since its replacement would disrupt the normal infectious ability of AAV, and thus the AAV-peptide fusion capsid will gain a new function originating from the nature of the grafted peptide. To explore the effect of exogeneous peptide insertion on the virus packaging and gene transduction ability, we first inserted a 12-residue peptide tag (PA tag, [23]) into the Cap of AAV serotype 2 (AAV2) at two locations (s1 and s2, Table S2) that had already been reported to tolerate a peptide

insertion (Fig. 2j)[24]. As expected, both mutant AAV2s (PA_s1-Cap^{AAV2} and PA_s2-Cap^{AAV2}) were efficiently produced in HEK cells at a titer comparable to the wildtype virus (Fig. 6a), indicating successful packaging of the gene-containing particles. On the other hand, the gene transduction activity was affected by the mutations, where the s1 mutant retained some activity compared to the wildtype particle whereas s2 mutant completely lost its activity (Fig. 6a). This deleterious effect of s2 modification on the AAV2 infectivity is likely due to the disruption of the binding to AAV2-specific receptor heparan sulfate proteoglycan [22] and/or the pan-AAV endocytosis receptor AAVR[25]. By using this PA_s2-Cap^{AAV2} incapable of infecting cells as a base capsid, we tested if presentation of m6A9 peptide on the capsid can mediate gene delivery into PlxnB1-expressing cells. Unfortunately, when the capsid was solely composed of the m6A9_s2-Cap^{AAV2}, the virus did not show satisfactory high titers (data not shown), suggesting its imperfect compatibility with the assembly of entire virus capsid and/or gene packaging. We therefore decided to employ a chimeric virus format, where only a fraction of capsid subunits was substituted with m6A9_s2-Cap^{AAV2}. By co-transfecting cells with plasmids coding for PA_s2-Cap^{AAV2} and m6A9_s2-Cap^{AAV2} at a DNA ratio of 9:1, a chimeric virus that likely incorporate up to six m6A9_s2-Cap^{AAV2} subunits per capsid was prepared. The resultant chimeric virus successfully transduced AcGFP gene into the Expi293F cells stably expressing human PlxnB1 (Fig. 6b), while no detectable AcGFP expression was observed with the parent cell line. We next expanded this analysis to another AAV serotype (AAV1) by using MET-binding aMD4 peptide as the targeting moiety. Unmodified AAV1 capsid was capable of transducing Chinese hamster ovary (CHO) cells or MET-overexpressing CHO cells (MET-CHO), while the mutant AAV1 composed of PA_s2-Cap^{AAV1} showed minimum transduction in both cells (Fig. 6c). In contrast, the chimeric AAV1 composed of 90% PA_s2-Cap^{AAV1} and 10% aMD4_s2-Cap^{AAV1} transduced AcGFP gene in a manner completely dependent on the presence of MET (Fig. 6c). In order to give more quantitative assessment as to the gene transduction capability of these receptor-oriented chimeric viruses, transduction of luciferase reporter gene was evaluated. As shown in Fig. 6d and e, dose-dependent luciferase induction into cells expressing PlxnB1 and MET was observed with the m6A9-grafted and aMD4-grafted chimeric viruses, respectively. Most importantly, they could not transduce parental cells devoid of the receptor expression, confirming the strict requirement of the target receptor of the grafted peptide for the infection.

Discussion

Emulating the natural immune system that can produce an almost infinite number of antibodies against yet-to-be encountered foreign molecules, various technology platforms to obtain artificial antibodies or antibody-like binder molecules toward specific target have been developed, exemplified by a broadly used phage-display method [26]. Although great conceptual and experimental variations exist among these technologies, they generally start with a library of proteins whose surface-exposed loop(s) are randomized, followed by a panning on the immobilized target molecule to select for specific binding clones. Arguably, these library-based selection methods represent the most successful cases in the modern biotechnology field that lead to the discovery of numerous useful biomolecules. However, the first-generation binders obtained from such partially randomized protein libraries often show modest level

of affinity due to the limited size of the library diversity, and it is often necessary to conduct additional selection campaigns for identifying improved binding clones worthy of the practical utility[27]. This second step usually involves directed evolution or saturation mutagenesis [28,29], and leads to a significant extension of development time and increase the uncertainty of the success.

The final products of our lasso-graft method reported here are similar to what would be obtained from the conventional methods described above in that they are all proteins with *de novo* loop sequences. However, the path to achieve this goal is totally different; we separated the “discovery” step involving selection and optimization of loop sequence via RaPID system from the “grafting” step that simply involves insertion of the optimized loop sequences into structurally permissive sites in a variety of protein scaffolds. In this way, one does not have to deal with difficulties in constructing library for a specific protein with randomized loop(s) each time, and take full advantage of the RaPID system which comprises a library of short (< 20-residue) cyclic peptides with more than 10^{12} diversity, leading to a rapid (generally within a few weeks) discovery of highly optimized binder peptides against target proteins at a remarkably high success rate. When a recombinant fusion of a biologically active peptide or peptides with a protein is desired, the primary fusion site is generally limited to either end. The “insertion” into an independently folded domain is considered as a risky approach due to the potential disturbance of the local structure. However, for peptides whose "active" structure (i.e., target-bound state) assume lasso-like conformation, loop-insertion often allows functional fusion [23,30]. In fact, such “binding-domain insertion” has been found in several natural antibodies where target-binding is mediated by small (~30 residues) to large (~100 residues) domain inserted at the tip of CDR3 loop [31,32].

One of the great advantages of the lasso-graft over existing grafting methods is the wide choice of scaffold proteins and grafting sites. As it has been known that heteromeric protein-protein interactions are often mediated by loops [33,34], a loop-grafting can be a promising way to transfer PPI onto unrelated proteins. However, only a limited number of special proteins are reported so far to be capable of presenting PPI-mediating loop peptides in an intact binding-competent conformation, and the grafting sites are also limited [35-37]. Choosing appropriate loop peptide moieties is also challenging, because flexible peptide conformation in isolation (i.e., detached from the target) is difficult to predict, and they tend to exhibit low affinity due to the entropic penalty upon binding [34]. We do not know exactly why RaPID-derived sequences show such high compatibility with the lasso-graft method, but suspect that the very high (> 10^{12}) diversity of the library enabled selection of very rare binder that assumes "self-folded" and "active" conformation before the encounter with the target. If the thioether-cyclized peptides can autonomously fold into a binding-competent conformation, the same conformation may be achieved by replacing the cyclizing bond with two closely apposed residues in the context of folded protein domain, regardless of the structure of the scaffold and insertion site.

Once a target-binding peptide sequence derived from a RaPID screening is confirmed to be compatible with lasso-grafting onto a certain protein, the same peptide motif can be “moved” to a desired location in the same or different proteins (Figure 3). The usefulness of this feature is best exemplified by its

application to the AAV capsid proteins. Unlike soluble globular proteins that exist in isolation (e.g., IgG and HSA), Cap proteins require their correct multisubunit assembly to maintain the native structure, which generally precludes a simple protein fusion unless the number and/or the sites of the fusion moiety are carefully controlled [21]. However, we believe that the lasso-graft approach introduces relatively small structural disturbance when applied to a surface-exposed and protruding loop, which contributed to the successful grafting of a PlxnB1- and MET-binding peptides onto the AAV2 and AAV1 particles in its binding-competent conformation. Importantly, the receptor-targeting moiety does not have to be presented in all 60 subunits in the capsid, and chimeric virus containing several peptide-bearing Cap subunits per particle was capable of transducing cells in a manner completely dependent on the receptor expression. Although AAV can infect and transduce broad range of cells/tissues through ubiquitously expressed sulfated glycans as well as the prerequisite endocytosis receptor AAVR, there is a need for the development of vectors that can only transduce limited type of tissues [24]. The present data suggest that the application of the lasso-graft approach to gene delivery vehicles including, but not limited to, AAV may enable usage of entry receptors arbitrary chosen from a large pool of cell surface molecules, to allow creation of custom-design vectors for gene therapy.

Lastly, the combinatorial capability is particularly important for the development of bi/multi-specific antibodies. Bispecific antibody is at the focus of intensive research due to its potential to target two disease-causing molecules at a time and/or to draw two antigens into a close proximity [38]. In addition to a conventional bispecific design of heterodimerized two half IgGs, numerous bi- and multi-specific antibody design modalities exist [17]. However, they tend to have issues in developability, immunogenicity, and manufacturability because of the highly engineered nature. In contrast, the addbody format we report here has minimum modification and maintains the global structure of the original IgG, leading to an instant development of quadruple-specific binder molecule without applying any special protein engineering know-how (Figure 5a). Considering the wide choice of the scaffold protein, we believe that the lasso-graft approach can expand the scope of the protein therapeutics beyond the current antibody-centered status.

Methods

Selection of the RaPID peptides

N-chloroacetyl-L- or D-Tyr-tRNA^{fMet} was prepared by the use of the respective amino acids esterified with cyanomethyl group (L- or D-ClAc-Tyr-CME) incubated with a flexizyme, eFx [39]. Ribosomal synthesis of the macrocyclic peptide library from NNK RNA templates was performed as previously described [40]. In brief, 1.2 μM puromycin-linked mRNA library was translated in a methionine deficient FIT reaction containing 25 μM either L- or D- ClAc-Tyr-tRNA^{fMet} for 30 min at 37 ˚C. The reaction was incubated at 25 ˚C for 12 min before disruption of the ribosome-mRNA complex by incubation at 37 ˚C for 30 min in the presence of 20 mM EDTA. The resulting peptide-linked mRNAs were then reverse transcribed using RNase H-reverse transcriptase (Promega) for 1 hour at 42 ˚C and buffer was exchanged for 50 mM Tris-HCl (pH

7.4), 150 mM NaCl, 0.05 vol% Tween-20. Affinity screening was performed by 3 serial passages (counter selections, 10 min each at 4 ˚C) of the library over Covalt-NTA or Streptavidin Dynabeads (Life Technologies), followed by affinity selection against 200 nM protein target immobilized on the same beads for 30 min at 4 ˚C. cDNA was eluted from the beads by heating to 95 ˚C for 5 min, and fractional recovery from the final counter selection (negative control) and the affinity selection step were assessed by quantitative PCR using Sybr Green I on a LightCycler thermal cycler (Roche). Enriched DNA libraries were recovered by PCR and used as input for transcription reactions to generate the mRNA library for the subsequent round of selection.

For high-throughput sequencing, DNA samples from the final round of selection were amplified, purified using a Nucleospin column (Machery-Nagel) and sequenced using a MiSeq high-throughput sequencer (Illumina). Data analysis was performed using CLC sequence viewer 7 software (Qiagen). The target proteins used to derive peptides described in this paper include biotinylated human PlxnB1 ectodomain [6], human MET ectodomain-Fc [5], biotinylated human EGFR ectodomain [41], His-tagged human TrkB ectodomain [Maini, submitted], and biotinylated human a6b1 integrin ectodomain [42].

Cell lines

Cell lines used in this study were obtained from ATCC (HEK293T, MDA-MB-231), RIKEN BRC Cell Bank (Jurkat), Thermo Fisher (Expi293F), and TAKARA bio (AAVpro 293T). Expi293F cells stably expressing human PlxnB1 [6] and CHO-K1 cells stably expressing human MET [43] were established previously. All cell lines were routinely tested for the presence of mycoplasma.

Protein design, construction, and expression

To design peptide-grafted proteins, each scaffold protein was structurally inspected to find appropriate insertion point where the Ca distance between the two anchorpoint residues located at chain ends (for dimer grafting, Fig.1a(i)) or within an exposed loop (for loop grafting, Fig.1a(ii)) were less than 7Å. Internal sequence of the RaPID-derived cyclic peptides (Table S1) were then inserted into these identified sites (Table S2) with up to three spacer residues of either Gly or Ser at both ends. All expression constructs were made using pcDNA3.1-based backbone with appropriate signal peptide and a tag or fusion partner to allow efficient purification and beads-pulldown assay. For the construction of the single-chain UG linked by the peptide (generally called UG_2-(*peptide name*)), two DNA fragments coding for human UG (UniProt P11684) and a peptide-coding region were assembled as shown in Figure S1a by extension PCR. For the construction of Fc-only protein, human IgG1 Fc (residues 104-330, UniProt P01857) was used without any tags. For Fc-fused b-sandwich domains, following regions were amplified from the original cDNAs or synthesized DNAs and fused with the human IgG1 Fc; residues 1539-1631 of human fibronectin (UniProt P02751-15); residues 35-142 of human CEA (UniProt P06731), residue 31-148 of human SIRPa (UniProt P78324), and residue 2-116 of anti-GFP single-domain antibody (PDB ID: 3OGO, [44]). Full length HSA (UniProt P02768), hGH (UniProt P01241), RBP (UniProt P02753), and ALP (UniProt P05187) coding regions were cloned in the pcDNA3.1 vectors with C-terminal His tag (HSA , hGHn and

ALP) or C-terminal PA tag [45](for RBP). Using these constructs as templates, peptide-inserted variants were prepared by extension PCR, followed by the verification of DNA sequences. For the construction of full-length IgG containing peptide grafts at the Fc region (i.e., addbody), the variable regions of heavy and light chains of YW64.3, avelumab, and OKT3 were gene-synthesized using the publicly available amino acid sequences and formulated in the form of human IgG1/kappa, and the peptide-insertion was performed as described above. For the addbodies containing more than one peptide insertions, the extension PCR process was repeated to incorporate different peptide sequences at different sites. Coding region of all expression constructs were verified by DNA sequencing. Protein expressions were performed using Expi293 expression system (Thermo Fisher) unless otherwise indicated. UG_2 proteins were purified from the culture supernatants using Ni-NTA-agarose resin as shown in Fig.S1b, buffer-exchanged to 20 mM Tris, 150 mM NaCl, pH 7.5 (TBS), concentrated to ~1 mg/ml, and stored at -80°C until used.

Beads pulldown

In order to assess the binding ability of various proteins grafted with m6A9 (PlxnB1 binder) or aMD4 (MET binder) in parallel, simple beads-pulldown method was utilized. To this end, soluble ectodomain fragments of human PlxnB1 (residues 1-535) and human MET (residues 1-931) with different tags were expressed and captured onto the beads immobilized with Protein A (for Fc-tagged version), anti-PA tag antibody NZ-1 (for PA-tagged version), or anti-MAP tag [30] antibody PMab-1 (for MAP-tagged version). After brief washing, the beads were further incubated with the culture supernatants containing various peptide-grafted proteins. Bound proteins were then eluted by adding SDS-containing buffer, and analyzed by SDS-PAGE. Binding specificity was confirmed by the lack of nonspecific binding of control scaffold proteins with no peptide insertions.

Kinetic binding measurement using Biacore (SPR)

The ectodomain fragments of human PlxnB1(1-535) or human MET(1-931) were biotinylated via BirA-mediated biosynthetic labeling using the protocol described previously [6], and immobilized onto a Series S sensor chip SA (GE Healthcare) at a surface density of ~930 RU (PlxnB1) and ~840 RU (MET), respectively. The binding was evaluated by injecting peptide-grafted UG solutions serially diluted using the running buffer (20 mM HEPES-NaOH (pH7.5), 150 mM NaCl, 0.05% Surfactant P20). The runs were conducted in a single cycle kinetics mode employing the following parameters; flow rate of 30 µl/min, contact time of 120 s, and dissociation time of 300 s. After each run, the surface was regenerated by injecting the regeneration buffer (10 mM Glycine-HCl (pH 3.0), 1M NaCl) until the response returned to the original baseline level. The binding curves of the measurement cell (immobilized with PlxnB1/MET) were subtracted with that of reference cell (unimmobilized), and used to derive kinetic binding values. Data were obtained using a Biacore T200 instrument (GE Healthcare) at 25°C, and the results were analysed by using Biacore T200 evaluation software version 4.1.

Flow cytometry

To measure binding of peptide-grafted Fc proteins to the respective target receptors, HEK 293T cells were transiently transfected with plasmids coding for various full-length human receptors including PlxnB1, MET, EGFR, TrkB, integrin a6b1, or Nrp1 using X-tremeGENE HP (Merck #6366236001), and detached from dishes by a brief treatment with trypsin/EDTA at 2 days post transfection, followed by an incubation with peptide-grafted Fc proteins diluted at ~10 μg/ml for 1.5 h. After washing twice with PBS, cells were incubated with AlexaFluor 488-labeled goat anti-human IgG (1:400 dilution, Thermo Fisher, A11013) at room temperature for 30 min. To measure binding of peptide-grafted IgG (addbodies), either the HEK293T transient transfectants or cell lines with endogenous expression of PD-L1 (MDA-MB-231), MET (MET-CHO), and CD3 (Jurkat) were used. Stained cells were analyzed on an EC800 system (Sony) and the data were analyzed with FlowJo software (Tomy Digital Biology).

Heterotypic cell-cell attachment assay

The CHO cells stably expressing human MET [43] were labeled by a fluorescent membrane marker DiI (Biotium, #30023) and plated in a 24-well plate (Thermo Fisher, #142475) at 5×10^5 cells/well in F12 growth medium containing 10% FCS. After 5 h, the cells were overlaid with Jurkat cells labeled by fluorescent membrane marker NeuroDiO (Biotium, #30021), which had been preincubated with purified OKT3 or aMD4-grafted OKT3 addbody at 5 μg/ml for 1.5 h on ice, and then further incubated for 30 min at 37 ºC. After removing the non-adherent Jurkat cells by gentle washing with ice-cold PBS for three times, the samples were fixed with 4% paraformaldehyde in PBS for 30 min at room temperature, and the phase-contrast and fluorescence cell images were recorded using TRITC filter set (for MET-CHO) and GFP filter set (for Jurkat) for at least 8 field views with a BZ-X700 digital fluorescence microscope (Keyence). The number of CHO cells (red fluorescence) and Jurkat cells (green fluorescence) cells were analyzed by using the hybrid cell count software (Keyence), and the average number of Jurkat cells attached per area were evaluated as the score of addbody-mediated heterotypic cell-cell attachment.

Recombinant production of AAV mutants and gene transduction assays

Recombinant AAV2 vector was prepared using an AAVpro Helper Free System (TAKARA, #6230). As the source of wild-type and mutant Cap subunits to prepare peptide-grafted AAV2 capsid, we modified the pRC2-mi342 plasmid encoding *Rep* and *Cap* genes. In order to avoid unwanted mutations introduced in this large (8.2 kb) plasmid, we first introduced unique AgeI and NheI sites flanking s1 and s2 sites to prepare pRC2-mi342AN. Various peptide insertion mutants were made on the ~0.8 kb AgeI-NheI fragment in a separate vector, and swapped into pRC2-mi342AN after sequence verification. As a result, pRC2-mi342AN plasmids with the following three mutations were constructed; PA_s1, PA_s2, and m6A9_s2. For the production of recombinant AAV1 vectors, pAAV2-1 plasmid carrying *Rep* gene from AAV2 and *Cap* gene from AAV1 (Addgene, #112862) was used. As in the case of AAV2 construction, mutations (PA_s2 and aMD4_s2) were introduced in the ~0.8 kb BsiWI-SbfI fragment in a separate vector before the final cloning in the pAAV2-1 plasmid. AAVpro-293T cell line (AAV-293, TAKARA, Z2273N) was used for AAV production and was cultured in 10% FCS/DMEM supplemented with 1 % non-essential amino acids (NEAA, Sigma, M7145-100mL) and 0.5 % penicillin/streptomycin (P/S, Sigma, P4458-100ML). AAV-293

cells were seeded at 8.0 × 10^5 cells/well in 6-well cell culture plate (Thermo Fischer, #24465). About 30 minutes before transfection, the culture medium was changed with 5 % FCS/DMEM containing 1 % NEAA and 0.5% P/S. Cells were transfected with 1 μg/well of a mixture of modified pRC2-mi342 or pAAV2-1 plasmids, 1 μg/well of pHelper plasmid, and 1 μg/well of pAAV-CMV-Fluc or pAAV-CAG-AcGFP plasmid (a kind gift from Takahisa Furukawa, Osaka University). Transfection was performed using 6 μg of PEI-Max (Polysciences, #24765-1). After 24 h post transfection, the culture medium was changed with 1 % FCS/DMEM supplemented with 1 % Glutamax (Gibco, #35050-061), 1 % NEAA and 0.5 % P/S. Seventy two hours after transfection, cells were collected and recombinant AAV was extracted using AAVpro extraction solution (TAKARA, #6235), and concentrated by ultrafiltration in PBS using Amicon ultra (Millipore, 100 kDa cutoff, UFC510024). Virus titers were determined by qPCR analysis of AAV genome copies using AAVpro titration kit ver. 2 (TAKARA, #6233). For the AcGFP gene transduction, Expi293F cells stably expressing human PlxnB1 [6] or the parental cells were seeded into each well of 96-well black wall plate (Greiner, #655090) at 5,000 cells/well and were infected with WT or mutant AAV2 at MOI = 6 × 10^5. Cells were cultured in 5 % FCS/DMEM including 1 % NEAA and 0.5 % P/S. In gene transduction with WT or mutant AAV1, CHO-K1 cells stably expressing human MET [43] or the parental cells were used and cultured in 5 % FCS/Ham's F12 (Wako, 087-08335) containing 0.5 % P/S. These cells were seeded at 10,000 cells/well and were infected at MOI = 5 × 10^4. Fluorescent microscope images were recorded after two days of infection by BZ-X700 microscope. For the luciferase gene transduction, cells were plated at 10,000 cells/well into 96-well black wall plate and cultured for one day, followed by infection with mutant AAV1s and AAV2s at MOI = 1.25 × 10^4, 2.5 × 10^4 and 5.0 × 10^4. Cells were cultured for additional 2 days in 5 % FCS/DMEM containing 1 % NEAA and 0.5 % P/S or 5 % FCS/Ham's F12 containing 0.5 % P/S, and the luciferase activity was determined by measuring luminescence for 0.5 second using Luciferase Assay System (Promega, E1501) in a Glomax NAVIGATOR (Promega, GM2000). Three or four technical replicates for each infection condition were measured.

Declarations

Author Contributions

E.M. performed and analyzed all the experiments with the exception of the following. S.W. performed and analyzed AAV experiments. N.K.B., R.M., Y.Y., and K.S. performed RaPID peptide selection against various receptors. N.N., Ky.M., and T.A. performed and analyzed UG-fusion experiments and Biacore experiments. Ku.M. supervised experiments on the MET-binder grafts and wrote the manuscript. H.S. and J.T. conceived the experimental design, analyzed the data and wrote the manuscript. All authors contributed to the preparation of the manuscript.

Competing interests

S.H. and J.T. are co-founders and shareholders of MiraBiologics Inc. E.M., K.S., and Ku.M. are also shareholders of the same company. All other authors declare no financial and non-financial competing interests.

Acknowledgements

We would like to thank Keiko Tamura-Kawakami for the construction of expression vectors. This work was supported in part by Japan Agency for Medical Research and Development (AMED), Platform Project for Supporting Drug Discovery and Life Science Research (Basis for Supporting Innovative Drug Discovery and Life Science Research) under JP19am0101090 and 19am0101075 to H.S. and J.T., respectively, Project for Cancer Research and Therapeutic Evolution (P-CREATE) from AMED to K.M., and by MEXT KAKENHI Grant Numbers 18K19298 from the Ministry of Education, Culture, Sports, Science and Technology of Japan (MEXT) to J.T.

References

1. Gao, M., Cheng, K. & Yin, H. Targeting protein-protein interfaces using macrocyclic peptides. *Biopolymers* **104**, 310–316, doi:10.1002/bip.22625 (2015).
2. Driggers, E. M., Hale, S. P., Lee, J. & Terrett, N. K. The exploration of macrocycles for drug discovery - an underexploited structural class. *Nat. Rev. Drug Discov.* **7**, 608–624, doi:10.1038/nrd2590 (2008).
3. Ito, K., Passioura, T. & Suga, H. Technologies for the synthesis of mRNA-encoding libraries and discovery of bioactive natural product-inspired non-traditional macrocyclic peptides. *Molecules* **18**, 3502–3528, doi:10.3390/molecules18033502 (2013).
4. Obexer, R., Walport, L. J. & Suga, H. Exploring sequence space: harnessing chemical and biological diversity towards new peptide leads. *Curr. Opin. Chem. Biol.* **38**, 52–61, doi:10.1016/j.cbpa.2017.02.020 (2017).
5. Ito, K. *et al.* Artificial human met agonists based on macrocycle scaffolds. *Nat. Commun.* **6**, 6373, doi:Artn 6373, 10.1038/Ncomms7373 (2015).
6. Matsunaga, Y., Bashiruddin, N. K., Kitago, Y., Takagi, J. & Suga, H. Allosteric inhibition of a semaphorin 4d receptor plexin b1 by a high-affinity macrocyclic peptide. *Cell Chem. Biol.* **23**, 1341–1350, doi:S2451-9456(16)30355-5 [pii] 10.1016/j.chembiol.2016.09.015 (2016).
7. Sakai, K. *et al.* Macrocyclic peptide-based inhibition and imaging of hepatocyte growth factor. *Nat. Chem. Biol.* **15**, 598–606, doi:10.1038/s41589-019-0285-7 (2019).
8. Song, X., Lu, L. Y., Passioura, T. & Suga, H. Macrocyclic peptide inhibitors for the protein-protein interaction of zaire ebola virus protein 24 and karyopherin alpha 5. *Org. Biomol. Chem.* **15**, 5155–5160, doi:10.1039/c7ob00012j (2017).

9. Otero-Ramirez, M. *et al.* Macrocyclic peptides that inhibit wnt signalling via interaction with wnt3a. *Royal society of chemistry*, 26–34, doi:10.1039/d0cb00016g (2020).
10. Vinogradov, A. A., Yin, Y. & Suga, H. Macrocyclic Peptides as Drug Candidates: Recent Progress and Remaining Challenges. *J. Am. Chem. Soc.* **141**, 4167–4181, doi:10.1021/jacs.8b13178 (2019).
11. Goto, Y. *et al.* Reprogramming the translation initiation for the synthesis of physiologically stable cyclic peptides. *ACS Chem. Biol.* **3**, 120–129, doi:10.1021/cb700233t (2008).
12. Suga, H. Max-Bergmann award lecture:A RaPID way to discover bioactive nonstandard peptides assisted by the flexizyme and FIT systems. *J. Pept. Sci.* **24**, doi:10.1002/psc.3055 (2018).
13. Mukherjee, A. B., Zhang, Z. & Chilton, B. S. Uteroglobin: a steroid-inducible immunomodulatory protein that founded the Secretoglobin superfamily. *Endocr. Rev.* **28**, 707–725, doi:10.1210/er.2007-0018 (2007).
14. Liang, W. C. *et al.* Function blocking antibodies to neuropilin-1 generated from a designed human synthetic antibody phage library. *J. Mol. Biol.* **366**, 815–829, doi:S0022-2836(06)01550-6 [pii] 10.1016/j.jmb.2006.11.021 (2007).
15. Boyerinas, B. *et al.* Antibody-dependent cellular cytotoxicity activity of a novel anti-pd-l1 antibody avelumab (msb0010718c) on human tumor cells. *Cancer Immunol. Res.* **3**, 1148–1157, doi:2326–6066.CIR-15-0059 [pii] 10.1158/2326–6066.CIR-15-0059 (2015).
16. Arakawa, F. *et al.* Cloning and sequencing of the vh and v kappa genes of an anti-cd3 monoclonal antibody, and construction of a mouse/human chimeric antibody. *J. Biochem.* **120**, 657–662, doi:10.1093/oxfordjournals.jbchem.a021462 (1996).
17. Labrijn, A. F., Janmaat, M. L., Reichert, J. M. & Parren, P. Bispecific antibodies: a mechanistic review of the pipeline. *Nat. Rev. Drug. Discov.* **18**, 585–608, doi:10.1038/s41573-019-0028-1 (2019).
18. Colella, P., Ronzitti, G. & Mingozzi, F. Emerging issues in aav-mediated in vivo gene therapy. *Mol. Ther. Methods Clin. Dev.* **8**, 87–104, doi:10.1016/j.omtm.2017.11.007 (2018).
19. Pillay, S. & Carette, J. E. Host determinants of adeno-associated viral vector entry. *Curr. Opin. Virol.* **24**, 124–131, doi:10.1016/j.coviro.2017.06.003 (2017).
20. Varadi, K. *et al.* Novel random peptide libraries displayed on aav serotype 9 for selection of endothelial cell-directed gene transfer vectors. *Gene Ther.* **19**, 800–809, doi:10.1038/gt.2011.143 (2012).
21. Munch, R. C. *et al.* Displaying high-affinity ligands on adeno-associated viral vectors enables tumor cell-specific and safe gene transfer. *Mol. Ther.* **21**, 109–118, doi:10.1038/mt.2012.186 (2013).
22. Dalkara, D. *et al.* In vivo-directed evolution of a new adeno-associated virus for therapeutic outer retinal gene delivery from the vitreous. *Sci. Transl. Med.* **5**, 189ra176, doi:10.1126/scitranslmed.3005708 (2013).
23. Fujii, Y. *et al.* Tailored placement of a turn-forming PA tag into the structured domain of a protein to probe its conformational state. *J. Cell Sci.*, 1512–1522, doi:10.1242/jcs.176685 (2016).

24. Grifman, M. *et al.* Incorporation of tumor-targeting peptides into recombinant adeno-associated virus capsids. *Mol. Ther.* **3**, 964–975, doi:10.1006/mthe.2001.0345 (2001).
25. Meyer, N. L. *et al.* Structure of the gene therapy vector, adeno-associated virus with its cell receptor, AAVR. *Elife* **8**, doi:10.7554/eLife.44707 (2019).
26. Clackson, T., Hoogenboom, H. R., Griffiths, A. D. & Winter, G. Making antibody fragments using phage display libraries. *Nature* **352**, 624–628, doi:10.1038/352624a0 (1991).
27. McCafferty, J. & Schofield, D. Identification of optimal protein binders through the use of large genetically encoded display libraries. *Curr. Opin. Chem. Biol.* **26**, 16–24, doi:10.1016/j.cbpa.2015.01.003 (2015).
28. Rocklin, G. J. *et al.* Global analysis of protein folding using massively parallel design, synthesis, and testing. *Science* **357**, 168–175, doi:10.1126/science.aan0693 (2017).
29. van Rosmalen, M. *et al.* Affinity Maturation of a Cyclic Peptide Handle for Therapeutic Antibodies Using Deep Mutational Scanning. *J. Biol. Chem.* **292**, 1477–1489, doi:10.1074/jbc.M116.764225 (2017).
30. Wakasa, A., Kaneko, M. K., Kato, Y., Takagi, J. & Arimori, T. Site-specific epitope insertion into recombinant proteins using the map tag system. *J. Biochem.*, doi:10.1093/jb/mvaa054 (2020).
31. Hsieh, F. L. & Higgins, M. K. The structure of a lair1-containing human antibody reveals a novel mechanism of antigen recognition. *Elife* **6**, doi:10.7554/eLife.27311 (2017).
32. Wang, F. *et al.* Reshaping antibody diversity. *Cell* **153**, 1379–1393, doi:10.1016/j.cell.2013.04.049 (2013).
33. Gavenonis, J., Sheneman, B. A., Siegert, T. R., Eshelman, M. R. & Kritzer, J. A. Comprehensive analysis of loops at protein-protein interfaces for macrocycle design. *Nat. Chem. Biol.* **10**, 716–722, doi:10.1038/NCHEMBIO.1580 (2014).
34. Der, B. S. & Kuhlman, B. Strategies to control the binding mode of de novo designed protein interactions. *Curr. Opin. Struct. Biol.* **23**, 639–646, doi:10.1016/j.sbi.2013.04.010 (2013).
35. Batori, V., Koide, A. & Koide, S. Exploring the potential of the monobody scaffold: effects of loop elongation on the stability of a fibronectin type III domain. *Protein Eng.* **15**, 1015–1020, doi:10.1093/protein/15.12.1015 (2002).
36. Rossmann, M., S, J. G., Moschetti, T., Dinan, M. & Hyvonen, M. Development of a multipurpose scaffold for the display of peptide loops. *Protein Eng. Des. Sel.* **30**, 419–430, doi:10.1093/protein/gzx017 (2017).
37. Madden, S. K., Perez-Riba, A. & Itzhaki, L. S. Exploring new strategies for grafting binding peptides onto protein loops using a consensus-designed tetratricopeptide repeat scaffold. *Protein. Sci.* **28**, 738–745, doi:10.1002/pro.3586 (2019).
38. Deshaies, R. J. Multispecific drugs herald a new era of biopharmaceutical innovation. *Nature* **580**, 329–338, doi:10.1038/s41586-020-2168-1 (2020).

39. Goto, Y., Katoh, T. & Suga, H. Flexizymes for genetic code reprogramming. *Nat. Protoc.* **6**, 779–790, doi:10.1038/nprot.2011.331 (2011).
40. Hayashi, Y., Morimoto, J. & Suga, H. In vitro selection of anti-Akt2 thioether-macrocyclic peptides leading to isoform-selective inhibitors. *ACS Chem. Biol.* **7**, 607–613, doi:10.1021/cb200388k (2012).
41. Yin, Y. *et al.* De novo carborane-containing macrocyclic peptides targeting human epidermal growth factor receptor. *J. Am. Chem. Soc.* **141**, 19193–19197, doi:10.1021/jacs.9b09106 (2019).
42. Miyazaki, N., Iwasaki, K. & Takagi, J. A systematic survey of conformational states in beta1 and beta4 integrins using negative-stain electron microscopy. *J. Cell Sci.* **131**, doi:10.1242/jcs.216754 (2018).
43. Miao, W. *et al.* Impaired ligand-dependent met activation caused by an extracellular sema domain missense mutation in lung cancer. *Cancer Sci.* **110**, 3340–3349, doi:10.1111/cas.14142 (2019).
44. Kubala, M. H., Kovtun, O., Alexandrov, K. & Collins, B. M. Structural and thermodynamic analysis of the GFP:GFP-nanobody complex. *Protein Sci.* **19**, 2389–2401, doi:10.1002/pro.519 (2010).
45. Fujii, Y. *et al.* PA tag: A versatile protein tagging system using a super high affinity antibody against a dodecapeptide derived from human podoplanin. *Protein. Expres. Purif.* **95**, 240–247, doi:Doi 10.1016/J.Pep.2014.01.009 (2014).
46. Unpublished **works** (manuscript copy attached as supplementary materials)
47. Nasir K. Bashiruddin, Mikihito Hayashi, Masanobu Nagano, Yan Wu, Yukiko Matsunaga, Junichi Takagi., Tomoki Nakajima, and Hiroaki Suga. Development of cyclic peptides with potent in vivo osteogenic activity through RaPID-based affinity maturation., submitted elsewhere.
48. Rumit Maini, Kota Tamada, Kunihiro Fukuda, Toru Takumi, and Hiroaki Suga. A de novo peptide that induces axonal growth through TrkB activation., submitted elsewhere.

Figures

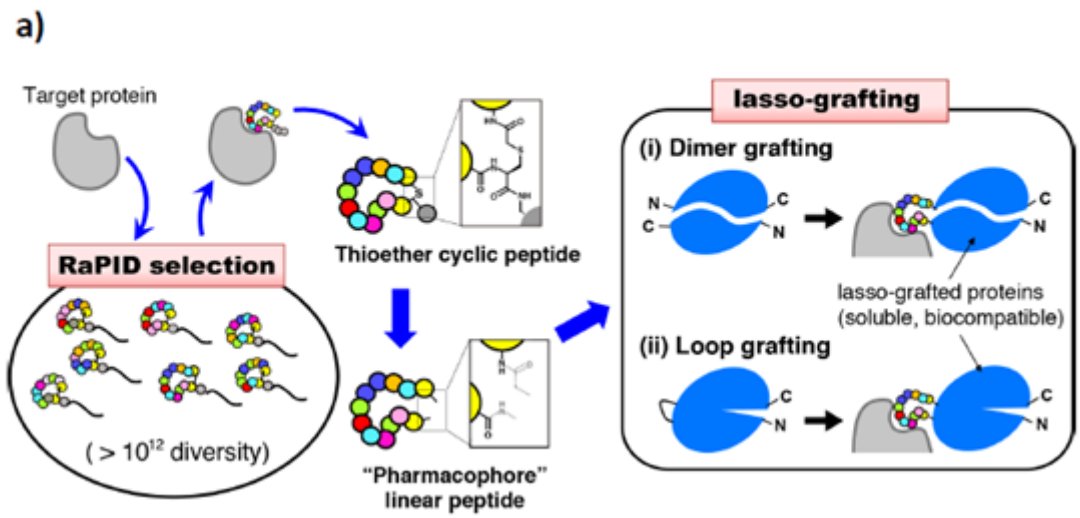

b)

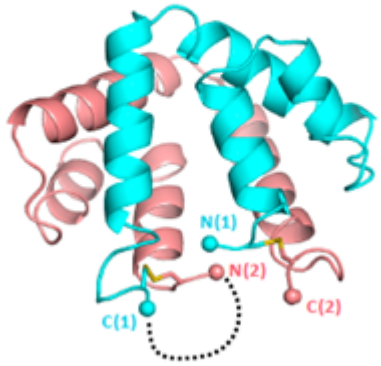

c)

analyte	kinetic constants		
	kon ($\mu M^{-1}s^{-1}$)	*koff* (s^{-1})	K_D (nM)
PB1m6 (free peptide)	3.46	0.012	3.5
PB1m6 (grafted on UG)	0.091	0.0041	45.8
PB1m6A9 (free peptide)	7.59	0.0021	0.28
PB1m6A9 (grafted on UG)	0.17	0.0014	8.26
PB1m7 (free peptide)	0.038	0.010	275
PB1m7 (grafted on UG)	0.0158	0.051	3250
aMD4 (free peptide)	1.4	0.003	2.4
aMD4 (grafted on UG)	0.044	0.004	91.6
aMD5 (free peptide)	4.8	0.011	2.3
aMD5 (grafted on UG)	0.088	0.019	211

Figure 1

Conversion of RaPID-derived cyclic peptides into protein grafts. a, Flow-chart of the lasso-graft method. Once high affinity cyclic peptide against a target is obtained via RaPID system in the discovery phase (left), the sequence information is used to formulate binding proteins in the grafting phase (right), either by inserting the peptide in between the N and C termini of homo/heterodimeric protein (i) or in the middle of an exposed loop of monomeric protein (ii). b, Disulfide-stabilized homodimeric structure of uteroglobin (PDB ID: 2UTG). Dotted line shows the position of peptide insertion between the C-terminus of molecule 1 (cyan) and N-terminus of molecule 2 (salmon). c, Kinetic binding constants for RaPID-derived peptides before and after the lasso-grafting. SPR binding of UG proteins grafted with PlxnB1-binding peptides (PB1m6, PB1m6A9, PB1m7) and MET-binding peptides (aMD4 and aMD5) toward respective target molecules are evaluated using Biacore (actual sensorgrams are shown in Figure S1c–h), followed by calculation of kinetic constants. Values for free peptides are taken from Matsunaga et al. 6 (for PB1m6 and PB1m7), Bashiruddin et al. (submitted) (for PB1m6A9), and Ito et al. 5 (for aMD4 and aMD5).

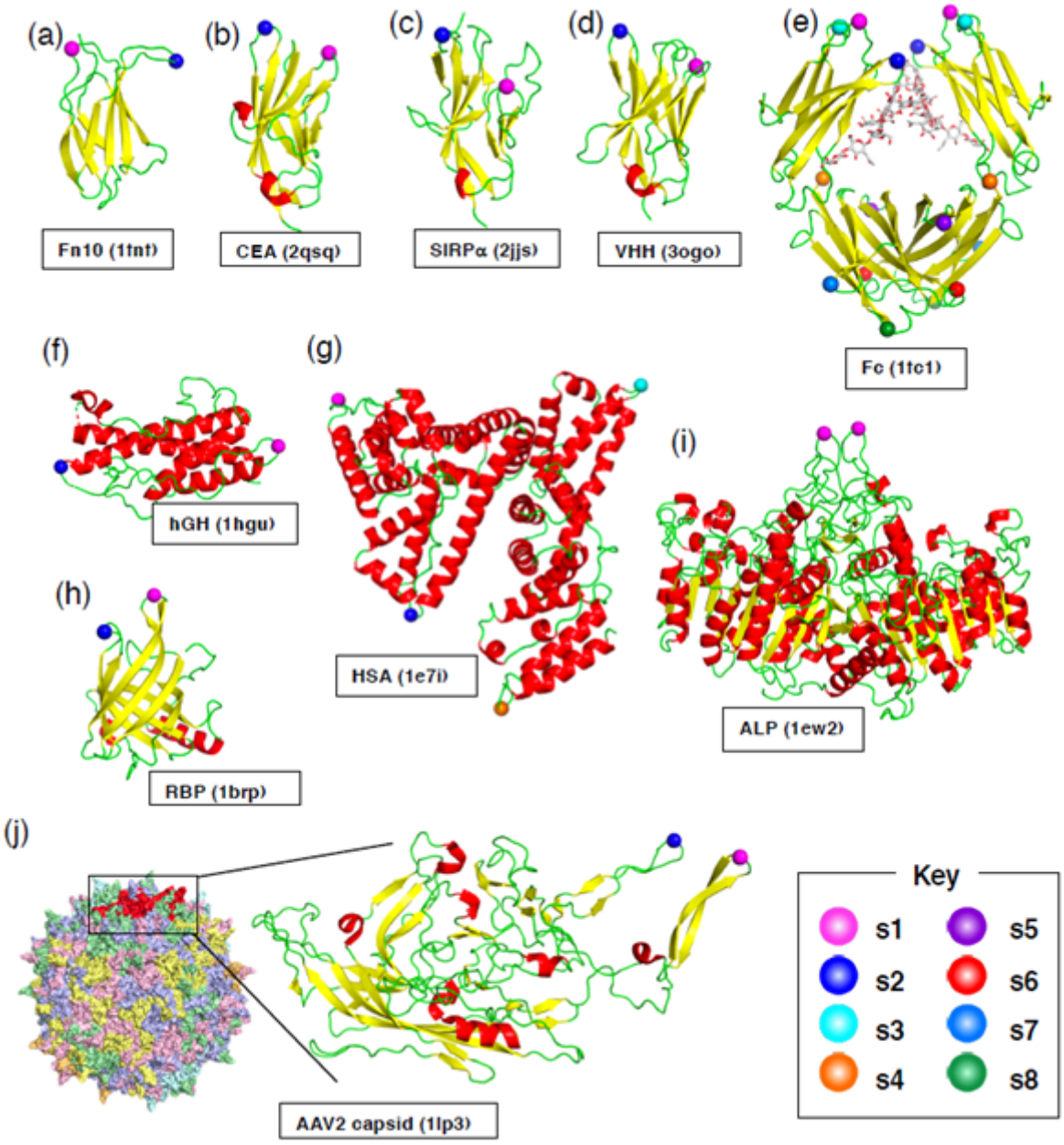

Figure 2

Location of the peptide insertion sites. Structure of following proteins or protein domains used as the grafting scaffold are shown in cartoon presentation; fibronectin 10th type-III domain (Fn10, PDB ID: 1FNF) (a), carcinoembryonic antigen (CEA, PDB ID: 2QSQ) 1st IgV domain (b), signal regulatory protein alpha (SIRPa, PDB ID: 2JJS) 1st IgV domain (c), anti-GFP single-domain antibody (VHH, PDB ID: 3OGO) (d), IgG1 Fc (PDB ID: 1FC1) (e), human growth hormone (hGH, PDB ID: 1HGU) (f), serum albumin (HSA, PDB ID: 1E7I) (g), retinol-binding protein (RBP, PDB ID: 1BRP) (h), placental alkaline phosphatase (ALP, PDB ID: 1EW2) (i), and VP3 capsid protein from AAV serotype 2 (PDB ID: 1LP3) (j). In (j), structure of the whole virus-like particle comprising 60 VP3 subunits is also shown, with each subunit differently colored. Insertion points are indicated by spheres with distinct colors shown in the key. Actual amino acid

sequence flanking the insertion sites are shown in Table S1. Note that two equivalent sites are present for each site in Fc and ALP, due to the homodimeric nature of these proteins.

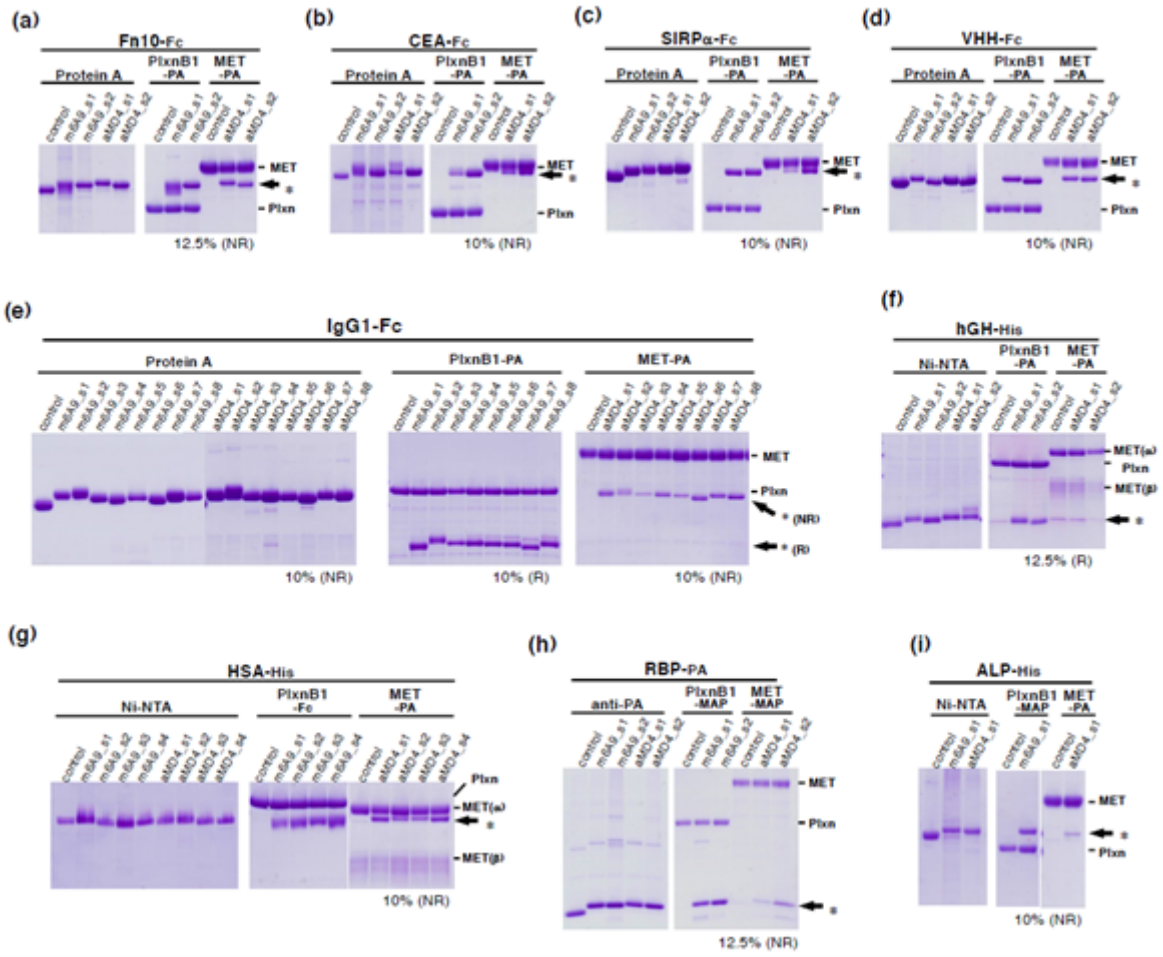

Figure 3

Lasso-grafting of binder peptides into various protein scaffolds. Nine different proteins or protein domains including Fn10-Fc (a), CEA-Fc (b), SIRPa-Fc (c), VHH-Fc (d), IgG1 Fc (e), hGH (f), HSA (g), RBP (h), and ALP (i) were grafted with m6A9 (PlxnB1-binder) or aMD4 (MET binder) peptides at different sites. Each graft design is denoted as peptide name_insertion site, e.g., m6A9_s4. Expression and secretion of these grafts, along with non-grafted proteins (control), were checked by pulldown experiments (left half of each panel) using beads immobilized with Protein A (for Fc-containing proteins, a-e), Ni-NTA (for His-tagged proteins, f, g, i), or anti-PA tag antibody NZ-1 (for PA-tagged proteins, h). The same set of samples are subjected to the pulldown using PlxnB1- or MET-captured beads (right half of each panel). For the capture strategy of differently tagged PlxnB1 and MET ectodomain fragments (including PA, MAP, and Fc), refer to the Methods section. Shown are Coomassie-stained, nonreducing(NR) SDS-PAGE gels of the beads-eluted proteins, except for some gels run under reducing (R) condition to avoid close migration of the grafted proteins with MET or Plxn. Acrylamide concentration of the gel and the running conditions (NR or R) are indicated at the bottom, and migration positions for MET, PlxnB1, and grafted proteins (*) are shown in the right.

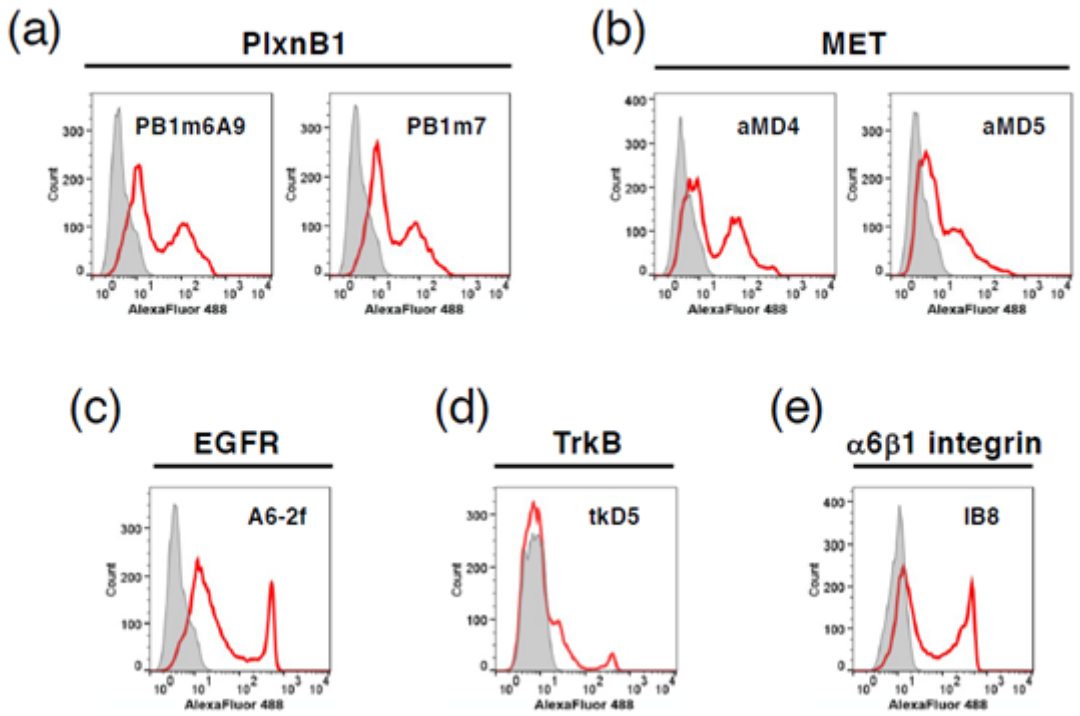

Figure 4

FACS binding analysis of various peptide-grafted Fc proteins to target receptors expressed on cell surface. HEK293T cells transiently expressing PlxnB1 (a), MET (b), EGFR (c), TrkB (d), or a6b1 integrin (e) are incubated with each peptide-Fc (red histogram) or control Fc (gray histogram), followed by staining with Alexa Fluor 488-labeled anti-human Fc.

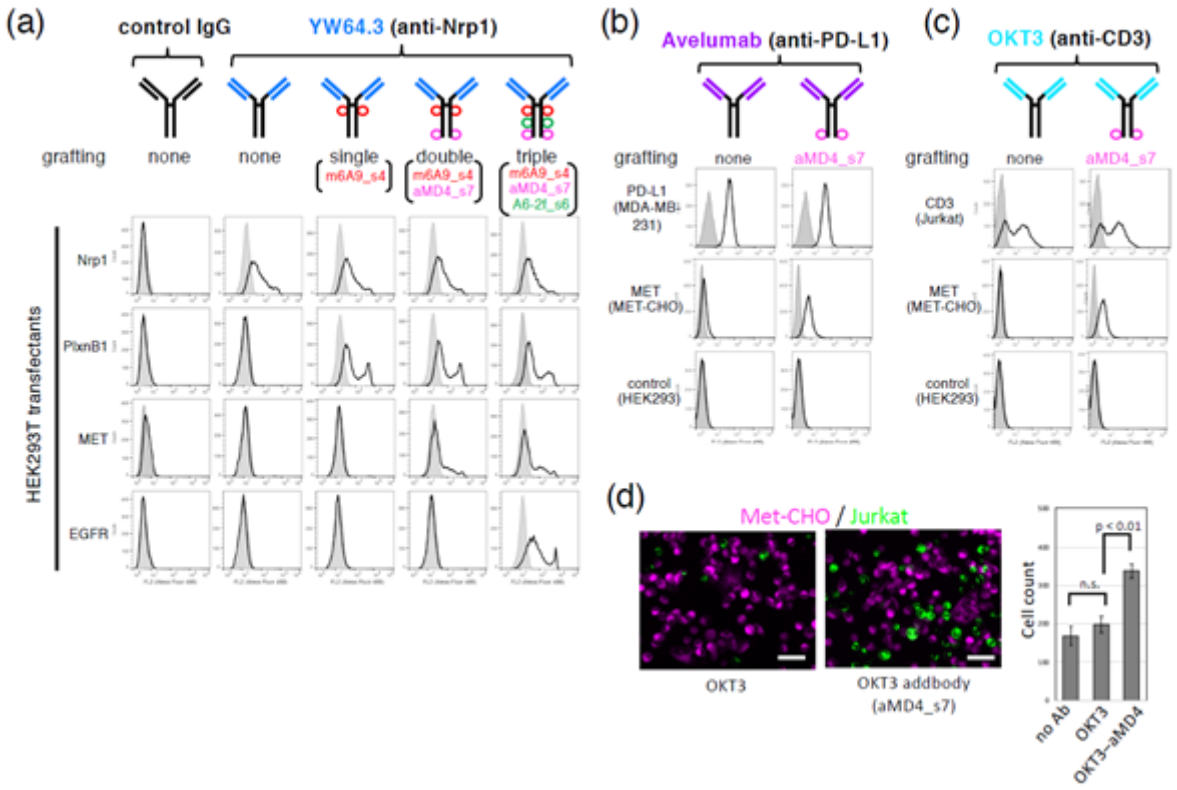

Figure 5

Instant formulation of multi-specific antibodies by peptide grafting onto IgG, addbodies. a-c, Flow cytometric binding analysis of variously grafted antibodies toward cells expressing antigens indicated on the left. Base antibodies include anti-neuropilin-1 YW64.3 (a), anti-PD-L1 avelumab (b), and anti-CD3 OKT3 (c). Each antibody design is schematically depicted above the panels. The gray histograms in (a) represent binding to untransfected HEK293T cells, while that in (b) and (c) are staining of the same cells with control IgG. d, Addbody-mediated heterotypic cell engagement. DiI-labeled MET-CHO cells (magenta) adhered onto the plate were overlaid with DiO-labeled Jurkat cells (green) in the presence of OKT3 (left) or OKT3- aMD4 addbody (right) and incubated for 30 min. After washing, the remaining cells were photographed (bar, 100 μm). Number of attached Jurkat cells were counted for multiple fields (n = 8) and shown in the right as mean ± SD (* P < 0.01, two-sided t-test; NS, not significant).

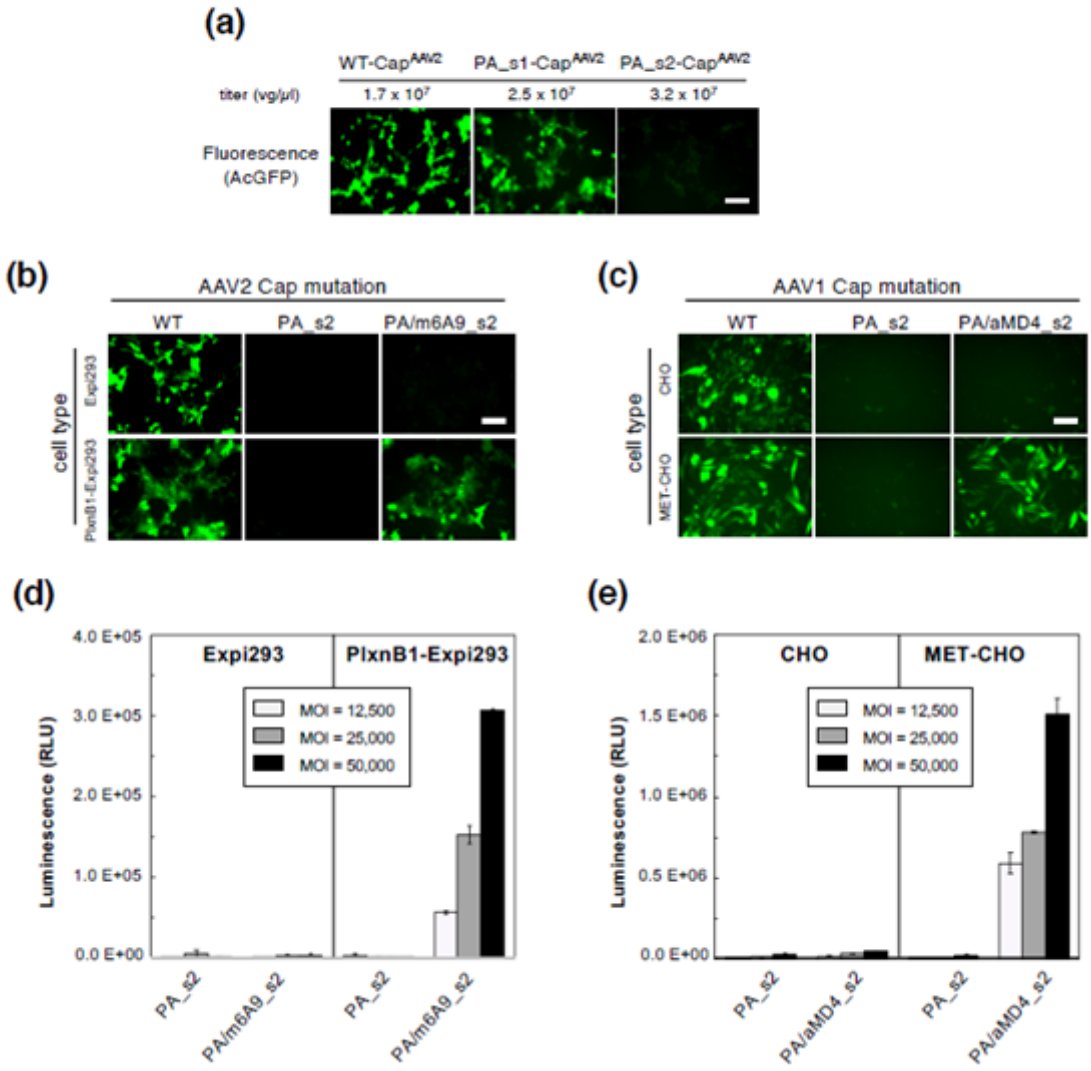

Figure 6

Peptide grafting onto AAV capsid enables acquisition of novel cellular tropism. a, Effect of PA tag insertion into the AAV2 Cap VP3 loops s1 and s2 on the capsid function. AcGFP-containing AAV2 with either wild-type (WT) or mutant capsids (PA_s1 and PA_s2) were recombinantly produced in AAVpro 293T cells and their titers were measured by qPCR. The virus stocks were then used to infect adherent Expi293F cells at MOI = 6 x 105 vg/cell. Fluorescent micrographs of the cells after 48 h of infection are shown. Scale bar, 100 μm. b, c, Receptor-dependent gene transduction with mutant AAV2 (b) or AAV1 (c). For PlexnB1- dependent transduction, cells stably expressing PlxnB1 or the parent cells were infected with wild-type (WT) or two mutant AAV2 particles containing AcGFP gene at MOI of 6 x 105 vg/cell, and photographed after 24h. For MET-dependent transduction, plain CHO cells or METoverexpressing CHO cells were infected with WT or mutant AAV1 particles at MOI of 5 x 104 vg/cell, and photographed after 48h. The PA_s2 mutant virus contains PA tag at the S2 site of all capsid subunits, while the chimeras (PA/m6A9_s2 or PA/aMD4_s2) contains PlxnB1- binding m6A9 peptide or MET-binding aMD4 peptide in ~10% of capsid subunits at the same site. Scale bar, 100 μm. d, e, Transduction with AAV-Luc. Indicated

cells were infected with AAV2 (d) or AAV1 (e) capsid mutants carrying luciferase reporter gene at varying MOI values, and analyzed for the luciferase activity after 48 h. Data are mean ± SD (n = 4 for d and n = 3 for e) from a representative experiment out of 9 (d) or 2 (e) independent ones.

Supplementary Files

This is a list of supplementary files associated with this preprint. Click to download.

- FigS1.png
- TableS1.png
- TableS2.png